Research Paper

JOURNAL OF MEDICO INFORMATICS

Molecular docking analysis of Naringenin from the leaves of Psidium guajava as a promising agent for breast cancer therapy

Murugesan Viji[1,2] | Subramanian Sathiya Jothi[3] | Krishnamoorthy Yasiha[3] | Sowntharrajan Aishwariya[1,2] | Christopher Ireen[1,2] | Sabapathy Indu[1,2] | Sekar Hinduja[2] | Manikkam Rajalakshmi[1,2,3] |

1. DBT-BIF Centre, Holy Cross College (Autonomous), Affiliated to Bharathidasan University, Tiruchirappalli, Tamil Nadu, India.
2. PG & Research Department of Biotechnology& Bioinformatics, Holy Cross College (Autonomous), Affiliated to Bharathidasan University, Tiruchirappalli, Tamil Nadu, India.
3. PG & Research Department of Zoology, Holy Cross College (Autonomous), Affiliated to Bharathidasan University, Tiruchirappalli, Tamil Nadu, India.

Abstract

Naringenin, a naturally occurring flavonoid isolated from *Psidium guajava* leaves, has been reported to exhibit multiple pharmacological properties, including antimicrobial, anti-inflammatory, antidiabetic, hepatoprotective, neuroprotective, cardioprotective, nephroprotective, anticancer, and antioxidant effects. Despite its wide pharmacological spectrum, its specific anticancer potential and molecular interactions against breast cancer targets remain underexplored. This study aimed to evaluate the drug-likeness, ADMET properties, and molecular docking profile of naringenin against critical breast cancer-associated proteins, including those involved in cell cycle regulation, apoptosis, oxidative stress, and NF-κB signaling. Naringenin was assessed for drug-likeness using Lipinski's Rule of Five and pharmacokinetic behavior through ADMET prediction tools. Molecular docking simulations were performed to analyze the binding affinities and interaction profiles between naringenin and selected target proteins such as CDK4, CDK6, catalase, Bcl-2, Bcl-xL, superoxide dismutase (SOD), glutathione peroxidase, and peroxiredoxin. Naringenin complied with the Lipinski rule of five and demonstrated favorable ADMET characteristics, suggesting good oral bioavailability and low toxicity risk. Molecular docking revealed that naringenin exhibited strong binding affinities, with the highest scores recorded against catalase (–10.3 kcal/mol), CDK4 (–8.3 kcal/mol), and CDK6 (–8.0 kcal/mol). Significant hydrogen bond interactions were observed with CDK4, Bcl-2, Bcl-xL, SOD, glutathione peroxidase, and peroxiredoxin, indicating its potential to modulate apoptotic and oxidative stress pathways relevant in breast cancer progression.

eJoMI2505

1. Introduction

Cancer encompasses nearly all cell types and represents a highly heterogeneous group of approximately 200 diseases characterized by a unifying hallmark: uncontrolled cellular proliferation leading to abnormal tissue growth. Among these malignancies, breast cancer remains one of the most prevalent cancers worldwide and constitutes a major cause of morbidity and mortality among women (Brown *et al.* 2023). Conventional therapeutic approaches, including surgery, chemotherapy, radiotherapy, hormonal therapy, targeted agents, and biological therapies, have significantly improved survival outcomes. However, these treatment modalities are often associated with substantial side effects, therapeutic resistance, and high relapse rates (Zafar *et al.* 2025). Consequently, there is a growing scientific interest in identifying safer and more effective alternatives from natural sources. Natural compounds with chemo preventive and chemotherapeutic potential are increasingly recognized as valuable candidates in anticancer drug discovery. *Psidium guajava* (guava), belonging to the family Myrtaceae, is a culturally and medicinally important tropical plant cultivated extensively across South America, India, Bangladesh, Pakistan, and Indonesia (Lok *et al.* 2023).

Various parts of the guava plant, including leaves, roots, bark, stems, and fruits, are traditionally used in ethnomedicine for treating ailments such as stomachache, diabetes, and diarrhea, underscoring its therapeutic value (Kumar *et al.* 2021). Naringenin [IUPAC name: 5,7-dihydroxy-2-(4-hydroxyphenyl) chroman-4-one], a flavanone abundantly present in grapefruits, oranges, tomatoes, and lemons, can be derived from the hydrolysis of glycosides such as naringin and narirutin (Salehi *et al.* 2019). It exists primarily in the aglycone form but also occurs in glycosylated and neohesperidoside derivatives. This compound (molecular weight: 272.25 g/mol; formula: C15H12O5) is soluble in polar organic solvents such as ethanol and dimethyl sulfoxide (Gao *et al.* 2024). Pharmacological investigations have highlighted its broad spectrum of bioactivities, including antimicrobial, anti-inflammatory, antidiabetic, hepatoprotective, neuroprotective, cardioprotective, nephroprotective, antioxidant, and anticancer effects (Cord, Rimbu, and Popescu 2025). Mechanistically, naringenin regulates oxidative stress by modulating reactive oxygen species (ROS) levels and enhancing antioxidant enzymes such as superoxide dismutase (SOD), thereby protecting cells against damage in cancers, chronic disorders, and metabolic diseases. Among phytochemicals with anticancer properties, naringenin is particularly noteworthy due to its unique dual functionality. It acts as a natural selective estrogen receptor modulator (SERM), functioning either as an agonist or antagonist depending on the cellular context, a property especially relevant in hormone-responsive malignancies such as breast cancer (Liou and Storz 2010). Additionally, naringenin disrupts key oncogenic signaling cascades, including the PI3K/Akt and MAPK/ERK pathways, which are frequently implicated in tumor growth, proliferation, and survival. This ability to simultaneously target hormone-dependent and non-hormonal signaling mechanisms is rare among plant-derived compounds, enhancing the therapeutic appeal of naringenin.

Furthermore, it has been reported to induce apoptosis, arrest cancer cell cycle progression, and exhibit minimal cytotoxic effects on normal cells, reinforcing its promise as a potential anticancer lead molecule (Lim *et al.* 2017). Previous studies have demonstrated its anticancer activity across multiple malignancies, including breast, gastric, colorectal, hepatic, cervical, leukemic, and pancreatic cancers. Considering these findings, the present study was designed to investigate the protein–ligand interactions of naringenin derived from *Psidium guajava* leaves with critical molecular targets implicated in breast cancer, focusing on proteins regulating the cell cycle, apoptosis, ROS signaling, and NF-κB pathways using an in-silico approach (Elsori *et al.* 2024).

Received on	:	08th July 2025	**Key Words:**
Revised on	:	28th July 2025	Naringenin
Accepted on	:	03rd August 2025	Docking
Published Online	:	07th September 2025	Breast cancer
Review Model	:	Single-Blind Review	*Psidium guajava*
No. of Reviewers	:	Two	Healthcare
Edited by	:	Dr. Chandrabose Selvaraj	Drug design
Vol and Issue	:	01 (01)	Public Health
Page No	:	35-43	
Plagiarism Level	:	11% and 15% (AI)	DOI: 10.64659/jomi/210351
Correspondence	:	Manikkam Rajalakshmi	**This article is licensed**
Contact Author	:	Rajalakshmi[at]hcctrichy.ac.in	CC BY-NC-ND

2. Materials and Method

2.1. Ligand Preparation

PubChem, a publicly accessible chemical information repository maintained by the National Institutes of Health (NIH), United States, provides comprehensive data on the chemical and biological properties of small molecules (Kim *et al.* 2016). The canonical SMILES of naringenin were retrieved from PubChem to ensure structural accuracy. The two-dimensional (2D) chemical structure of the ligand was subsequently generated and illustrated using ACD/ChemSketch (Jiang *et al.* 2023).

2.2. Drug-Likeliness Properties

The pharmacokinetic profile of naringenin was evaluated using *in silico* approaches. Drug-likeness was assessed based on Lipinski's Rule of Five parameters, including molecular weight, hydrogen bond donors, hydrogen bond acceptors, and lipophilicity (Demian *et al.* 2024). Additionally, absorption, distribution, metabolism, excretion, and toxicity (ADMET) properties were predicted using the pkCSM pharmacokinetics platform, which employs graph-based signatures to model compound behavior and provide insights into gastrointestinal absorption, blood–brain barrier permeability, cytochrome P450 interactions, renal clearance, and potential toxicities (Pires, Blundell, and Ascher 2015).

2.3. Determination of Lipinski Rule

Another fundamental aspect of computational drug discovery is the evaluation of drug-likeness using Lipinski's Rule of Five. This rule serves as a guideline for predicting the absorption and permeability of compounds across biological membranes (Karami *et al.* 2022). According to Lipinski's criteria, a compound is more likely to exhibit favorable oral bioavailability if it meets at least four of the following parameters: (i) molecular weight ≤ 500 g/mol, (ii) octanol–water partition coefficient (log P) < 5, (iii) no more than five hydrogen bond donors, and (iv) no more than ten hydrogen bond acceptors, primarily nitrogen and oxygen atoms. Compounds adhering to these parameters are generally considered drug-like and are more suitable for further pharmacokinetic and pharmacological evaluations (Ahmad *et al.* 2023).

2.4. Determination of Data of ADMET

A comprehensive evaluation of absorption, distribution, metabolism, excretion, and toxicity (ADMET) properties is indispensable in the discovery and development of novel therapeutic agents. These parameters play a central role in determining the pharmacokinetic behavior, safety, and overall drug-likeness of candidate molecules (Jung *et al.* 2024). *In silico* prediction of ADMET characteristics provides a rapid, cost-effective, and preliminary assessment prior to experimental validation, thereby reducing the need for extensive early-stage in vitro and in vivo testing. This approach is particularly advantageous for identifying potential liabilities, as newly synthesized compounds may possess unforeseen toxicities (Venkataraman *et al.* 2025). In the present study, ADMET predictions were performed using the pkCSM web-based platform, which employs graph-based signatures of chemical structures to systematically calculate and analyze pharmacokinetic and toxicity profiles (Ghayoor and Kohan 2024).

2.5. Protein Preparation

The three-dimensional (3D) crystal structures of selected protein targets associated with breast cancer were retrieved from the Protein Data Bank (PDB). These included: Cell cycle regulatory proteins: Cyclin-D1 (PDB ID: 2W99_A), Cyclin-D3 (PDB ID: 3G33_B), Cyclin-dependent kinase 4 (CDK4; PDB ID: 3G33_A), Cyclin-dependent kinase 6 (CDK6; PDB ID: 1G3N_A), Cyclin-dependent kinase inhibitor 4c (p18INK4c; PDB ID: 1G3N_B), Cyclin-dependent kinase inhibitor 1 (p21WAF1/CIP1; PDB ID: 1AXC_B), and Cyclin-dependent kinase inhibitor 1B (p27KIP1; PDB ID: 1JSU_C) (Goodger *et al.* 1997). Apoptotic proteins: B-cell lymphoma-extra-large (Bcl-xL; PDB ID: 1G5J_A), B-cell leukemia/lymphoma 2 (Bcl-2; PDB ID: 1G5M_A), Caspase-3 (apoptosis-execution protease; PDB ID: 1GFW_A), Caspase-9 (apoptosis-initiating protease; PDB ID: 1NW9_B), Caspase-6 (apoptosis-execution protease; PDB ID: 2WDP_A), Caspase-8 (apoptosis-initiating protease; PDB ID: 5JQE_A), Bcl-2-associated X protein (Bax; PDB ID: 2K7W_B), and Bcl-2 antagonist/killer (Bak; PDB ID: 2YV6_A) (Saleem *et al.* 2013). Reactive oxygen species (ROS)-related proteins: Catalase (CAT; PDB ID: 1QQW_A), Superoxide dismutase (SOD; PDB ID: 1SPD_A), Glutathione peroxidase-2 (GPx-2; PDB ID: 2HE3_A), and Peroxiredoxin (PDB ID: 1OC3_A) (Moloney and Cotter 2018). NF-κB pathway proteins: NF-κB p52 subunit (PDB ID: 1A3Q_A), NF-κB p65 subunit (PDB ID: 1NFI_A), and NF-κB p100 subunit (PDB ID: 3DO7_B) (Yu *et al.* 2020). All receptor structures were preprocessed using BIOVIA Discovery Studio Visualizer 2021 Client. The preparation involved removal of crystallographic water molecules, nucleic acid residues, native ligands, and heteroatoms, followed by the addition of polar hydrogen atoms to optimize receptor geometry and improve potential receptor–ligand interactions during docking (Li, Jiang, and Yang 2022).

2.6. Grid Box Generation

Grid box generation is a critical step in molecular docking as it delineates the spatial boundaries within which the ligand is allowed to explore potential binding conformations on the target protein. In this study, the grid box was configured to fully encompass the active site of each receptor. The grid dimensions were set to 25 × 25 × 25 Å, and the center coordinates were manually assigned based on the position of key active-site residues (Meng *et al.* 2011). These residues were identified either by referencing the co-crystallized ligand present in the protein structures or through binding pocket prediction analysis. This strategy ensured comprehensive coverage of the functionally relevant binding region, thereby enhancing the reliability of receptor–ligand interaction predictions. The chosen grid parameters were optimized to achieve a balance between docking accuracy and computational efficiency (Lopez, Ezkurdia, and Tress 2009).

2.7. Molecular Docking

Molecular docking simulations were conducted using PyRx version 0.8, which integrates AutoDock Vina as its default docking engine. Prior to docking, all ligand molecules were energy-minimized using the Open Babel module embedded within PyRx to optimize structural geometries and reduce steric clashes. The docking protocol was executed with AutoDock Vina's default settings, with the exhaustiveness parameter set to 8, ensuring an optimal balance between computational efficiency and conformational sampling (Alamri *et al.* 2020). Docking outcomes were evaluated based on binding affinity scores, reported as Vina scores in kcal/mol, where more negative values correspond to stronger predicted binding interactions (Wong *et al.* 2022). To assess the robustness of the docking workflow, validation was performed by re-docking the native co-crystallized ligand into the corresponding receptor's active site. The predicted binding conformations were compared with the crystallographic poses using Root Mean Square Deviation (RMSD) analysis, with an RMSD value of ≤ 2.0 Å considered indicative of reliable and reproducible docking accuracy (Mukherjee, Balius, and Rizzo 2010).

2.7. Protein-Ligand Interaction Studies

The docking poses were further analyzed to characterize the key molecular interactions stabilizing the ligand–protein complexes. Specific interactions, including hydrogen bonding, hydrophobic contacts, and π–π stacking, were identified and visualized using the BIOVIA Discovery Studio Visualizer 2021 Client software (Vinod *et al.* 2023). Both 2D and 3D interaction profiles were generated, enabling a detailed examination of

the binding conformations. Interaction maps included parameters such as bond types and bond lengths, which provided insights into the strength and spatial orientation of the ligand–receptor interactions. This analysis facilitated the identification of critical residues within the active site that contributes to the binding affinity and specificity of naringenin toward its target proteins (Anwar *et al*. 2024).

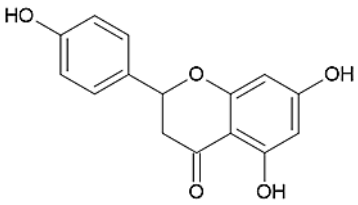

Figure 1. 2D Structure of Naringenin

3. Results

3.1. Chemistry of Naringenin

Naringenin ($C_{15}H_{12}O_5$) is a naturally occurring flavanone belonging to the flavonoid family and is widely distributed in citrus fruits. Structurally, it is composed of two aromatic rings (A and B) linked through a three-carbon heterocyclic ring (C), which contains a chiral center at the C-2 position **(Figure 1)**. The molecule bears three hydroxyl groups located at C-5 and C-7 on the A ring and at C-4′ on the B ring, which contribute to its antioxidant properties. Naringenin occurs both as a free aglycone and in glycosylated forms, such as naringin. Its conjugated aromatic system and phenolic moieties enable it to function as a hydrogen donor, metal chelator, and free radical scavenger. Additionally, the planar core structure promotes π–π stacking interactions, while the hydroxyl substitution pattern influences its solubility, chemical reactivity, and spectrum of biological activities. Pharmacologically, naringenin has been reported to exhibit anti-inflammatory, antioxidant, anticancer, hepatoprotective, and other therapeutic effects.

Table 1. Naringenin-LIPINSKI rule of 5

Ligand	Naringenin
Molecular Weight	272.256
LogP	2.5099
Rotatable bonds	1
Acceptors	5
Donors	3
Surface area	114.235

Table 2. ADMET properties of Naringenin.

ADMET Properties	Naringenin
Internal absorption (Human) (% Absorbed)	91.31
BBB permeability (log BB)	-0.578
CYP2D6 substrate	No
CYP2D6 inhibitor	No
Total clearance (log ml/min/kg)	0.06
AMES toxicity	No
Oral Rat Acute Toxicity (LD50) (mol/kg)	1.791
Oral Rat Chronic Toxicity (LOAEL)	1.944
Hepatotoxicity	No

3.2. Lipinski's Rule of Five

The drug-likeness assessment of naringenin was conducted using Lipinski's Rule of Five and comprehensive i*n silico* ADMET profiling, collectively demonstrating its potential as an orally bioavailable therapeutic candidate for breast cancer treatment. Naringenin exhibits favorable molecular descriptors that fully satisfy Lipinski's criteria: molecular weight of 272.256 Da (≤500 Da), LogP value of 2.5099 (<5), one rotatable bond (optimal flexibility), five hydrogen bond acceptors (≤10), and three hydrogen bond donors (≤5). Furthermore, its polar surface area (PSA) of 114.235 Ų falls within the optimal range (≤140 Ų) that favors passive membrane permeability and gastrointestinal absorption, supporting its suitability for oral drug delivery **(Table 1)**.

Table 3. Binding affinity and H-bond interactions of Naringenin with cell cycle proteins.

Proteins	Binding affinity (kcal/mol)	H-bond interactions	Other interactions with bond length
Cyclin D1	-6.9	LYS A:180(2.03Å) GLN A:183(2.78Å)	PRO A:79 (5.45Å) ALA A:187(4.27Å)
Cyclin D3	-6.6	ARG B:87(2.20Å) CYS B:91(2.84Å)	LEU B:148 (3.53Å) ARG B:37 (4.79Å) ARG B:41 (4.50Å)
CDK4	-8.3	GLU A:99 (2.89Å) HIS A:100(2.18Å) VAL A:101(2.11Å) ASP A:163(2.64Å)	LEU A:152 (3.71Å) ALA A:38 (4.81Å) ILE A:17(4.43Å) ASP A:104(3.30Å)
CDK6	-8.0	-	ASP A:163(3.36Å) LEU A:76(3.78Å) TYR A:24(3.89Å)
P18 INK4c	-6.4	GLN B:93(2.92Å) ALA B:127(2.18 Å)	LEU B:90(4.56Å) VAL B:96(5.41Å)
P21 CIP1	-4.9	GLN B:144 (2.04 Å)	PHE B:150(3.71Å) MET B:147 (5.20Å)
P27 KIP1	-5.7	TYR C:88(3.09Å)	LEU C:84 (5.34Å) VAL C:79 (4.79Å)

Table 4. Binding affinity and H-bond interactions of Naringenin with apoptotic proteins.

Proteins	Binding affinity (kcal/mol)	H-bond interactions	Other interactions with bond length
Bcl-xL	-7.4	LEU A:198(2.83Å) ARG A:104(2.64Å) SER A:207(2.89Å)	ALA A:203 (4.32Å) ALA A:97 (4.33Å) VAL A:145 (5.22Å) TYR A:199 (3.73Å)
Bcl-2	-7.5	ASP A:196(2.42Å) TRP A:195(2.74Å) ASN A:182(2.06Å) ASN A:11 (2.77Å)	ILE A:189 (5.36Å) GLY A:194 (2.92Å)
Caspase 3	-6.1	ARG A:147 (2.27Å)	PHE A:142 (3.98Å)
Caspase 9	-6.8	ASN B:265 (2.52Å) GLY B:277 (2.34Å)	ILE B:341 (4.89Å) GLY B:276 (3.57Å)
Bax	-5.1	GLY B:156 (2.81Å)	ASN B:160 PHE B:159 (4.16Å)
Caspase 6	-7.7	LYS A:133 (2.37Å)	ILE A:136 (5.18Å) ALA A:162 (3.67Å) TYR A:210 (5.41Å) GLU A:214(4.26Å) LEU A:200 (3.88Å)
Bak	-7.4	-	ILE A:114 (5.26Å) PRO A:102 (4.99Å) HIS A:99 (5.01Å) LEU A:97 (3.79Å)
Caspase 8	-7.5	SER A:1004 (2.15Å)	LEU A:1042(3.77Å) ALA A:350 (4.16Å) PRO A:346(4.20Å) GLN A:347

3.3. ADMET Properties

The ADMET predictions further substantiate naringenin's pharmacological viability as a therapeutic agent. The compound demonstrates excellent gastrointestinal absorption with a predicted

human intestinal absorption rate of 91.31%, indicating efficient uptake following oral administration. Its blood–brain barrier (BBB) permeability value of −0.578 suggests limited central nervous system penetration, which is advantageous for minimizing potential neurological adverse effects when treating peripheral malignancies such as breast cancer. Metabolic stability assessments reveal that naringenin is predicted to function neither as a substrate nor as an inhibitor of the CYP2D6 isoenzyme, thereby reducing the likelihood of clinically significant drug–drug interactions and metabolic complications. The compound exhibits moderate systemic clearance with a total clearance rate of 0.06 mL/min/kg, which may contribute to sustained plasma concentrations and prolonged therapeutic effects. Toxicological profiling indicates a favorable safety margin across multiple endpoints. Naringenin tested negative for AMES mutagenicity and hepatotoxicity and demonstrated acceptable thresholds for both acute oral toxicity (LD_{50} = 1.791 mol/kg) and chronic exposure (LOAEL = 1.944 log mg/kg-bw/day) in rat models. Collectively, these pharmacokinetic and safety parameters establish that naringenin satisfies the essential criteria for drug development, supporting its advancement as a lead compound for preclinical breast cancer research **(Table 2)**.

Table 5. Binding affinity and H-bond interactions of Naringenin with ROS proteins.

Proteins	Binding affinity (kcal/mol)	H-bond interactions	Other interactions with bond length
Superoxide dismutase	-6.6	GLU A:132(2.98Å) THR A:135(2.70Å) HIS A:63(2.31Å)	LYS A:136(5.07Å) LYS A:70 (5.18Å) PRO A:62 (5.49Å) ARG A:69(3.54Å)
Catalase	-10.3	THR A:361 (2.41Å)	ALA A:133 (4.88Å) ARG A:72 (3.58Å) HIS A:75 (4.22Å)
Glutathione peroxidase-2	-6.5	ARG A:184 (2.00Å TYR A:125 (2.08Å) ARG A:168 (1.91Å)	LEU A:123 (3.78Å) ARG A:167(3.40Å)
Peroxiredoxin	-6.7	ARG A:86(2.08Å VAL A:94(2.07Å) GLY A:92(2.55Å)	ALA A:90 (5.29Å) GLY A:82(3.54Å)

Table 6. Binding affinity and H-bond interactions of Naringenin with NF-κB Subunit proteins.

Proteins	Binding affinity (kcal/mol)	H-bond interactions	Other interactions with bond length
NF-κB/p52	-6.5	LEU A:117(2.01 Å)	ILE A:119 (3.83Å) LYS A:153 (4.32 Å) ALA A:104 (4.91 Å) ARG A:160 (4.47Å) ARG A:103 (4.26Å)
NF-κB/p65	-6.9	GLN A:119(2.32Å)	LYS A:37 (3.81Å) LYS A:122 (4.86 Å) VAL A:121 (4.75Å) ARG A:124 (4.55Å)
NF-κB/p100	-7.5	ARG B:103 (2.90Å) GLN B:157 (2.99Å) LEU B:117 (2.58Å)	ALA B:104(4.26Å) LYS B:153 (4.27Å) GLY B:118 (3.34Å)

3.4. Molecular Docking

Molecular docking represents a fundamental technique of *in silico* approach for predicting ligand–protein interactions and estimating binding affinities, serving as an essential preliminary screening tool in drug discovery pipelines (Pinzi and Rastelli **2019**). Binding affinities, typically expressed in kcal/mol by docking platforms such as AutoDock Vina, provide quantitative insights into interaction strength, with more negative values indicating stronger predicted binding. Generally, binding affinities of ≤ −6.0 kcal/mol are considered moderate, while values ≤ −8.0 kcal/mol suggest strong binding potential and likely biological relevance (Antypenko *et al.* **2025**). However, docking predictions are subject to inherent limitations, including scoring function approximations, limited protein flexibility modeling, and incomplete solvation considerations. These factors contribute to typical error margins of ±2.0 kcal/mol in binding affinity predictions, necessitating cautious interpretation of results (Jain **2009**). To validate docking reliability, root means square deviation (RMSD) analysis is employed, where RMSD values ≤ 2.0 Å between predicted and crystallographic ligand poses confirm protocol accuracy. While molecular docking enables rapid screening of extensive compound libraries, integration with molecular dynamics simulations and experimental validation is recommended to substantiate binding predictions and pharmacological significance (Ramirez and Caballero **2018**). The selected protein targets represent critical nodes in cell cycle regulation, apoptotic control, oxidative stress response, and transcriptional signaling pathways frequently dysregulated in breast cancer progression. Cell Cycle Regulatory Proteins: Cyclins D1 and D3, in association with their catalytic partners CDK4 and CDK6, drive G1/S phase transition through retinoblastoma (Rb) protein phosphorylation, promoting cellular proliferation (Pellarin *et al.* **2025**). Overexpression of these complexes is frequently observed in various malignancies, contributing to uncontrolled growth.

Conversely, cyclin-dependent kinase inhibitors including p18INK4c, p21CIP1, and p27KIP1 function as tumor suppressors by negatively regulating CDK activity, inducing cell cycle arrest and constraining proliferation. Apoptotic Pathway Proteins: The balance between pro- and anti-apoptotic proteins determines cellular fate (Schirripa, Sexl, and Kollmann **2022**). Anti-apoptotic proteins Bcl-2 and Bcl-xL maintain mitochondrial membrane integrity and prevent cytochrome c release, while pro-apoptotic proteins Bax and Bak promote mitochondrial outer membrane permeabilization, activating the intrinsic apoptotic cascade. This process sequentially activates Caspase-9 (initiator) and Caspase-3 (executioner), culminating in programmed cell death through substrate cleavage (Carrington *et al.* **2017**). Oxidative Stress Response Proteins: Reactive oxygen species (ROS) exhibit dual roles in carcinogenesis, moderate levels promote tumorigenesis, while excessive ROS can trigger apoptosis. Antioxidant enzymes including Catalase, Superoxide Dismutase (SOD), Glutathione Peroxidase (GPx), and Peroxiredoxin maintain redox homeostasis by neutralizing ROS (Xu *et al.* **2017**). Dysregulation of these protective mechanisms sensitizes cells to oxidative damage and apoptotic induction. NF-κB Signaling Components: The NF-κB pathway serves as a pivotal regulator of cell survival and inflammatory responses. The canonical pathway involves NF-κB/p65, while the non-canonical pathway encompasses NF-κB/p52 and NF-κB/p100 subunits. Constitutive NF-κB activation in malignancies promotes transcription of anti-apoptotic and pro-proliferative genes, whereas pathway inhibition sensitizes tumor cells to therapeutic intervention (Liu *et al.* **2017**).

Naringenin demonstrated robust interactions with key cell cycle proteins, including Cyclin D1 (−6.9 kcal/mol), Cyclin D3 (−6.6 kcal/mol), CDK4 (−8.3 kcal/mol), and CDK6 (−8.0 kcal/mol) **(Table 3)**. The strongest affinity was observed with CDK4, where naringenin formed multiple hydrogen bonds and hydrophobic interactions, suggesting a high probability of effectively inhibiting cell cycle progression. Moderate binding was also seen with p18INK4c (−6.4 kcal/mol), p21CIP1 (−4.9 kcal/mol), and p27KIP1 (−5.7 kcal/mol), reflecting its versatility in engaging tumor suppressor proteins. The ligand exhibited strong binding affinities to anti-apoptotic proteins Bcl-2 (−7.5 kcal/mol), Bcl-xL (−7.4 kcal/mol), and pro-apoptotic effectors such as Bak (−7.4 kcal/mol) and caspase 6 (−7.7 kcal/mol) **(Table 4)**. These interactions were stabilized by numerous

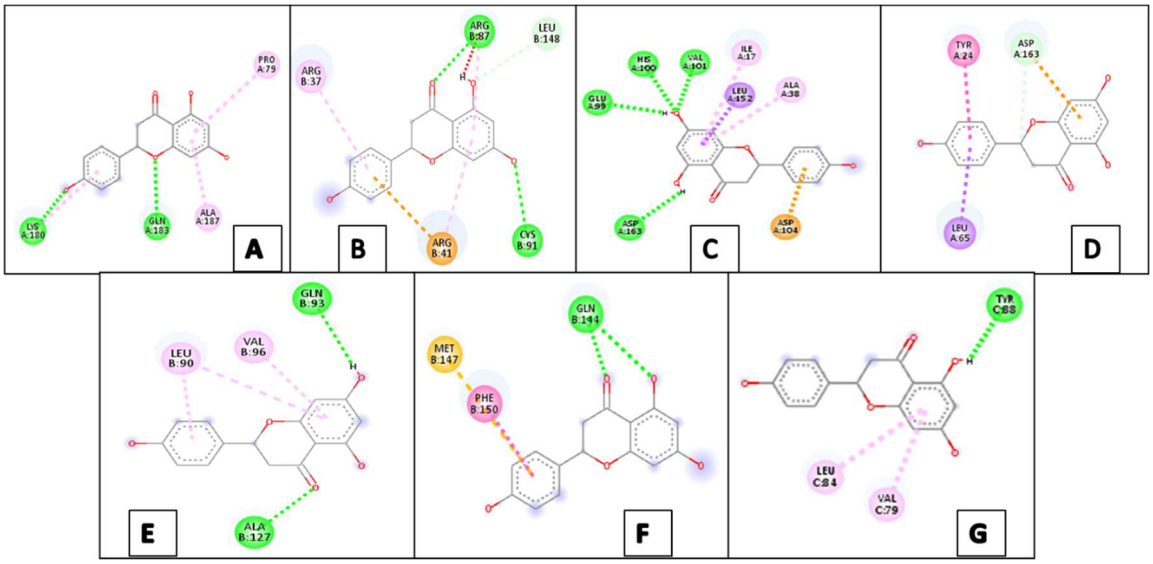

Figure 2. Molecular interaction between Naringenin and cell cycle proteins such as Cyclin D1, Cyclin D3, CDK4, CDK6, p18 INK4c, p21 CIP1 and p27 KIP1.

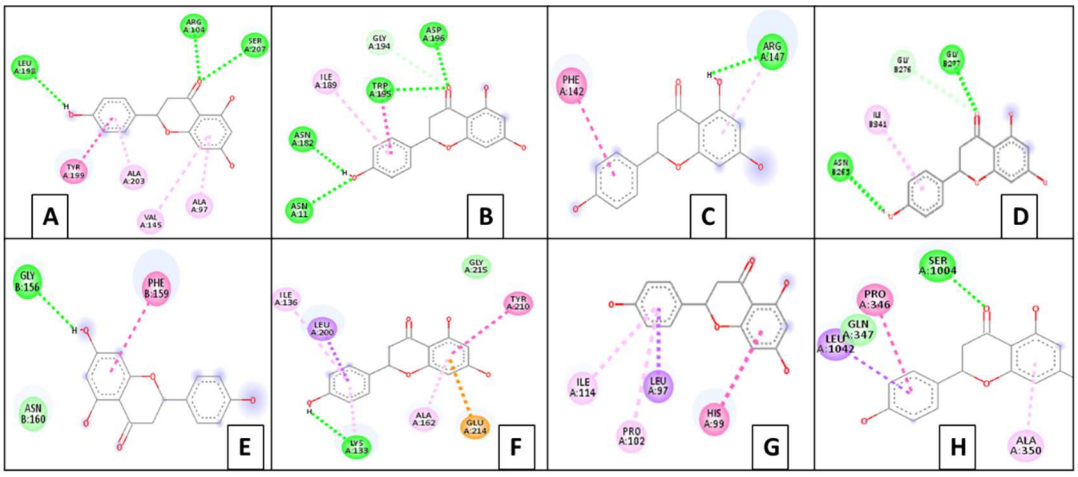

Figure 3. Molecular interaction between Naringenin and apoptotic proteins such as Bcl-xL, BCL-2, Caspase 3, Caspase 9, Bax, Caspase 6, Bak and Caspase 8.

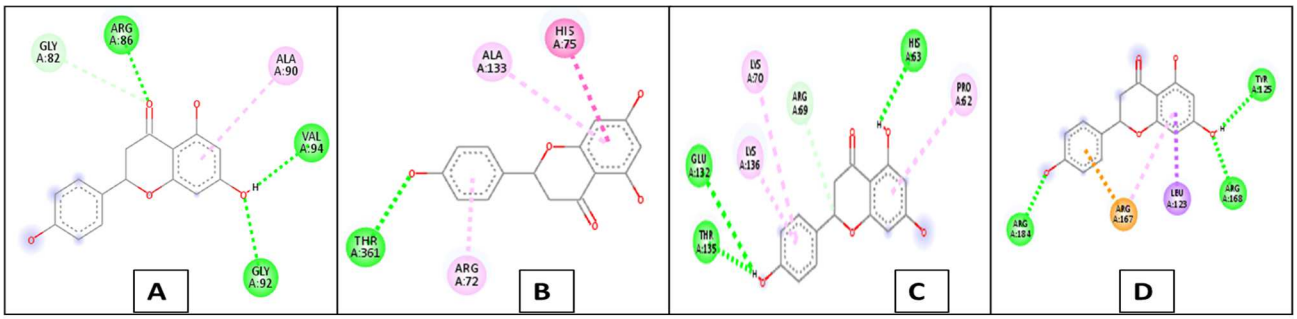

Figure 4. Molecular interaction between Naringenin and ROS proteins such as Peroxiredoxin, Catalase, Superoxide dismutase and Glutathione peroxidase-2.

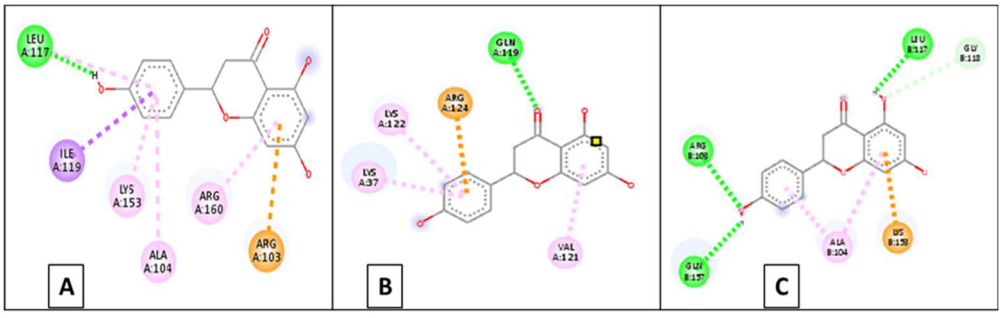

Figure 5. Molecular interaction between Naringenin and NF-κB proteins such as NF-κB/p52, NF-κB/p65 and NF-κB/p100.

hydrogen bonds, π–π stacking, and hydrophobic contacts, signifying naringenin's ability to modulate apoptosis pathways both by inhibiting survival signals and promoting programmed cell death in cancer cells. A particularly strong binding affinity was observed with catalase (–10.3 kcal/mol), highlighting naringenin's potential to target mitochondrial oxidative stress defenses. Substantial interactions were also established with superoxide dismutase (–6.6 kcal/mol), glutathione peroxidase-2 (–6.5 kcal/mol), and peroxiredoxin (–6.7 kcal/mol) **(Table 5)**. These findings suggest a mechanism for naringenin that involves modulation of redox balance and possibly sensitizing cancer cells to oxidative damage. The compound presented notable binding affinities with NF-κB subunits, including p52 (–6.5 kcal/mol), p65 (–6.9 kcal/mol), and p100 (–7.5 kcal/mol) **(Table 6)**. The molecular interactions comprised hydrogen bonding and several hydrophobic/aromatic contacts, indicating naringenin's capacity to interfere with transcriptional activity involved in cell survival, proliferation, and inflammation.

3.5. Molecular Interactions

3.5.1. Naringenin with Cell Cycle Regulatory Proteins

Naringenin demonstrates notable binding affinities and diverse molecular interactions with several cell cycle proteins implicated in cancer progression **(Figure 2)**. For Cyclin D1, naringenin achieved a binding affinity of –6.9 kcal/mol and formed hydrogen bonds with LYS A:180 (2.03 Å) and GLN A:183 (2.78 Å). Additional stabilization was conferred through pi-alkyl interactions involving PRO A:79 (5.45 Å) and ALA A:187 (4.27 Å), enhancing its fit within the protein's active site. With Cyclin D3, naringenin showed a binding affinity of –6.6 kcal/mol, establishing hydrogen bonds with ARG B:87 (2.20 Å) and CYS B:91 (2.84 Å). The ligand further engaged in carbon-hydrogen bond interaction with LEU B:148 (3.53 Å), along with pi-alkyl and pi-cation interactions involving ARG B:37 (4.79 Å) and ARG B:41 (4.50 Å), respectively, indicating robust contact with key residues. A pronounced binding affinity of –8.3 kcal/mol was observed for CDK4, the strongest among assessed targets. Naringenin established multiple hydrogen bonds with GLU A:99 (2.89 Å), HIS A:100 (2.18 Å), VAL A:101 (2.11 Å) and ASP A:163 (2.64 Å), as well as diverse non-covalent interactions including pi-sigma (LEU A:152, 3.71 Å), pi-alkyl (ALA A:38, 4.81 Å; ILE A:17, 4.43 Å), and pi-anion (ASP A:104, 3.30 Å), reflecting a highly stabilized and specific docking pose. For CDK6, naringenin also showed a high binding affinity (–8.0 kcal/mol), featuring carbon-hydrogen bond interaction (ASP A:163, 3.36 Å) along with pi-sigma (LEU A:76, 3.78 Å) and π-π stacked (TYR A:24, 3.89 Å) interactions, supporting effective engagement with the protein's interface.

With p18INK4c, a binding affinity of –6.4 kcal/mol was measured; hydrogen bonds were formed with GLN B:93 (2.92 Å) and ALA B:127 (2.18 Å), alongside pi-alkyl (LEU B:90, 4.56 Å and 5.36 Å; VAL B:96, 5.41 Å) interactions, indicative of multi-point anchoring. Naringenin displayed moderate binding to p21CIP1 (–4.9 kcal/mol), involving hydrogen bonds with GLN B:144 (2.04 Å, 2.58 Å), as well as π-π stacked (PHE B:150, 3.71 Å) and pi-sulfur (MET B:147, 5.20 Å) interactions, suggesting a less optimal but diverse interaction profile. For p27KIP1, naringenin's binding affinity was –5.7 kcal/mol, coupled with a hydrogen bond to TYR C:88 (3.09 Å), and stabilization through pi-alkyl interactions (LEU C:84, 5.34 Å; VAL C:79, 4.79 Å).

3.5.2. Naringenin with Apoptotic Proteins

Naringenin exhibits strong binding affinities and forms multiple stabilizing interactions with a range of apoptotic proteins, integral to the regulation of programmed cell death in cancer **(Figure 3)**. For Bcl-xL, the compound achieved a binding affinity of –7.4 kcal/mol, establishing hydrogen bonds with LEU A:198 (2.83 Å), ARG A:104 (2.64, 2.87 Å), and SER A:207 (2.89 Å). The ligand's fit was further strengthened by pi-alkyl interactions (ALA A:203, 4.32 Å; ALA A:97, 4.33 Å; VAL A:145, 5.22 Å) and a π-π stacking interaction (TYR A:199, 3.73 Å). Similarly, for Bcl-2, naringenin displayed a binding affinity of –7.5 kcal/mol, engaging in hydrogen bonds with ASP A:196 (2.42 Å), TRP A:195 (2.74 Å), ASN A:182 (2.06 Å), and ASN A:11 (2.77 Å). Additional stabilizing contacts included a pi-alkyl interaction (ILE A:189, 5.36 Å) and a carbon–hydrogen bond (GLY A:194, 2.92 Å). With caspase 3, naringenin demonstrated a moderate binding affinity of –6.1 kcal/mol, forming a hydrogen bond with ARG A:147 (2.27 Å) and engaging in a π-π stacking interaction (PHE A:142, 3.98 Å). For caspase 9, the binding affinity was –6.8 kcal/mol, featuring hydrogen bonds with ASN B:265 (2.52 Å) and GLY B:277 (2.34 Å), as well as pi-alkyl (ILE B:341, 4.89 Å) and carbon–hydrogen (GLY B:276, 3.57 Å) interactions. Interaction with Bax yielded a binding affinity of –5.1 kcal/mol, highlighted by a hydrogen bond with GLY B:156 (2.81 Å), van der Waals contact (ASN B:160), and an amide–pi stacked interaction (PHE B:159, 4.16 Å). Naringenin's binding to caspase 6 was notably strong (–7.7 kcal/mol), featuring hydrogen bonding (LYS A:133, 2.37 Å), pi-alkyl (ILE A:136, 5.18 Å; ALA A:162, 3.67 Å), amide–pi stacking (TYR A:210, 5.41 Å), pi-anion (GLU A:214, 4.26 Å; 4.64 Å), van der Waals (GLY A:215), and pi-sigma (LEU A:200, 3.88 Å) interactions. For Bak, naringenin showed a binding affinity of –7.4 kcal/mol, supported by pi-alkyl (ILE A:114, 5.26 Å; PRO A:102, 4.99 Å), π-π stacking (HIS A:99, 5.01 Å), and pi-sigma (LEU A:97, 3.79 Å) interactions. Against caspase 8, the compound exhibited a strong binding affinity (–7.5 kcal/mol) with hydrogen bonding (SER A:1004, 2.15 Å), pi-sigma (LEU A:1042, 3.77 Å), pi-alkyl (ALA A:350, 4.16 Å), amide–pi stacking (PRO A:346, 4.20 Å, 5.40 Å), and van der Waals (GLN A:347) contacts.

3.5.3. Naringenin with ROS-Modulating Proteins

Naringenin demonstrates notable binding affinities and distinct interaction profiles with reactive oxygen species (ROS)-related antioxidant enzymes, supporting its potential role in modulating cellular redox balance **(Figure 4)**. For superoxide dismutase (SOD), naringenin exhibits a binding affinity of –6.6 kcal/mol, forming hydrogen bonds with GLU A:132 (2.98 Å), THR A:135 (2.70 Å), and HIS A:63 (2.31 Å). The docking was further stabilized by pi-alkyl interactions involving LYS A:136 (5.07 Å), LYS A:70 (5.18 Å), and PRO A:62 (5.49 Å), complemented by a carbon–hydrogen bond with ARG A:69 (3.54 Å). With catalase, naringenin exhibited an exceptionally strong binding affinity of –10.3 kcal/mol. Key interactions included a hydrogen bond with THR A:361 (2.41 Å), pi-alkyl interactions with ALA A:133 (4.88 Å) and ARG A:72 (3.58 Å), and π-π stacking interaction with HIS A:75 (4.22 Å), suggesting highly favorable stabilization within the enzyme's active pocket. For glutathione peroxidase-2 (GPx-2), the ligand demonstrated a binding affinity of –6.5 kcal/mol, making hydrogen bonds with ARG A:184 (2.00 Å, 2.76 Å), TYR A:125 (2.08 Å), and ARG A:168 (1.91 Å). Further multi-modal contacts included a pi-sigma interaction (LEU A:123, 3.78 Å) and a pi-cation interaction (ARG A:167, 3.40 Å). Naringenin's interaction with peroxiredoxin resulted in a binding affinity of –6.7 kcal/mol. Stabilizing contacts comprised hydrogen bonds with ARG A:86 (2.08 Å, 2.45 Å), VAL A:94 (2.07 Å), and GLY A:92 (2.55 Å), together with a pi-alkyl interaction (ALA A:90, 5.29 Å) and carbon–hydrogen bond (GLY A:82, 3.54 Å).

3.5.4. Naringenin with NF-κB Subunit Proteins

Naringenin demonstrates substantial binding affinity and diverse intermolecular interactions with NF-κB subunit proteins, which are pivotal in regulating cell survival, inflammation, and oncogenic signaling **(Figure 5)**. For NF-κB/p52, the ligand exhibits a binding affinity of –6.5 kcal/mol and establishes a hydrogen bond with LEU A:117 (2.01 Å). The stability of the complex is enhanced by pi-sigma interaction (ILE A:119, 3.83 Å), multiple pi-alkyl interactions involving LYS A:153 (4.32 Å), ALA

A:104 (4.91 Å), and ARG A:160 (4.47 Å), and a pi-cation interaction with ARG A:103 (4.26 Å), collectively indicating strong anchoring within the protein's functional domain. Against NF-κB/p65, naringenin demonstrates a slightly higher binding affinity (–6.9 kcal/mol), forming a hydrogen bond with GLN A:119 (2.32 Å). The binding is further stabilized by pi-alkyl interactions (LYS A:37, 3.81 Å; LYS A:122, 4.86 Å; VAL A:121, 4.75 Å), and a pi-cation interaction (ARG A:124, 4.55 Å), implying robust intermolecular recognition and stabilization. With NF-κB/p100, naringenin achieves its highest affinity among these subunits (–7.5 kcal/mol), forming hydrogen bonds with ARG B:103 (2.90 Å), GLN B:157 (2.99 Å), and LEU B:117 (2.58 Å). The ligand also engages in pi-alkyl interactions (ALA B:104, 4.26 Å & 4.76 Å), pi-cation interactions (LYS B:153, 4.27 Å), and carbon–hydrogen bond interactions (GLY B:118, 3.34 Å), together promoting optimized binding at critical regulatory sites. In total, naringenin not only met key thresholds for binding energy but also demonstrated diverse stabilizing interactions,hydrogen bonds, π–π stacking, pi-alkyl contacts, and cation–π associations,with critical proteins implicated in breast cancer biology. These results strongly support its candidacy as a multi-pathway modulator with potential for further development as an anticancer agent targeting cell cycle, apoptosis, oxidative stress, and NF-κB signaling pathways.

4. Discussion

Naringenin, a naturally derived flavanone, has garnered significant attention due to its diverse pharmacological profile and promising drug-like properties. Its distinctive chemical structure, comprising two aromatic rings and a three-carbon heterocyclic ring with a chiral center, imparts a variety of physicochemical attributes, such as the ability to donate hydrogen, chelate metals, and scavenge free radicals. The positions and number of hydroxyl groups further influence naringenin's antioxidant activity, solubility, reactivity, and therapeutic potential, which is validated by its occurrence both as a free aglycone and as glycosides in nature. Widely distributed in citrus fruits, naringenin serves as a lead compound for the development of molecules with anti-inflammatory, anticancer, and hepatoprotective benefits. Comprehensive evaluation based on Lipinski's Rule of Five indicates naringenin's pronounced suitability for oral administration. The compound meets all key parameters: a moderate molecular weight (272.256 Da), favorable lipophilicity (LogP 2.5099), optimal flexibility, and correct numbers of hydrogen bond donors and acceptors.

With a polar surface area conducive to passive diffusion across biological membranes, naringenin is predicted to possess efficient gastrointestinal absorption. This is further substantiated by *in silico* ADMET profiling, which confirms a high predicted human absorption rate (91.31%) and a moderate total clearance, supporting sustained systemic exposure. Notably, limited blood–brain barrier permeability suggests reduced likelihood of neurological side effects, particularly important in non-CNS cancers. Additionally, naringenin's predicted metabolic stability (non-interaction with CYP2D6) and favorable toxicological profile (negative for mutagenicity and hepatotoxicity) further reinforce its candidacy for drug development and preclinical testing. The molecular docking analyses offer mechanistic insights into naringenin's interactions with key proteins that drive breast cancer progression and therapy resistance. With cell cycle regulatory proteins such as Cyclin D1, CDK4, and CDK6, naringenin forms stable complexes through both hydrogen bonding and hydrophobic contacts, particularly with strong binding affinities to CDK4 and CDK6.

These interactions have the potential to disrupt aberrant cell cycle progression, a hallmark of cancer biology. Naringenin's binding with apoptotic proteins, including Bcl-xL, Bcl-2, and various caspases, proved similarly favorable. Extensive hydrogen bonding and stacking interactions suggest its ability to modulate both intrinsic and extrinsic apoptotic pathways, thereby reinforcing programmed cell death in malignant cells.

In the context of oxidative stress, naringenin displays high affinity for key antioxidant enzymes such as catalase, superoxide dismutase, glutathione peroxidase, and peroxiredoxin. This multi-target engagement underscores its role in maintaining redox balance and protecting cells against ROS-induced damage, an established mechanism of cancer prevention and therapy. Particularly notable is its robust interaction with catalase, suggesting a strong propensity to intervene in oxidative stress responses.

The compound's molecular interactions with NF-κB subunit proteins reveal its potential to disrupt abnormal transcriptional activity, cell survival, and inflammation. Binding to both canonical (p65) and non-canonical (p52, p100) subunits, with multiple hydrogen bonds and hydrophobic contacts, positions naringenin as a candidate NF-κB pathway modulator, a strategic point for anticancer intervention. Collectively, these findings demonstrate that naringenin possesses a combination of favorable drug-likeness, pharmacokinetic properties, and broad-spectrum target engagement, addressing multiple cancer-relevant biological processes. The diverse and pronounced molecular interactions revealed through docking studies suggest the compound's utility as a multi-target lead, supporting its further development in preclinical breast cancer therapeutics.

5. Conclusion

This *in silico* investigation robustly demonstrates that naringenin possesses key drug-like characteristics and a favorable pharmacokinetic profile, underpinning its potential as a multitarget agent for breast cancer therapy. Its molecular framework, featuring polyphenolic groups and a planar structure, enables strong antioxidant activity and versatile biological interactions. Naringenin fully satisfies Lipinski's Rule of Five and exhibits excellent predicted absorption, low risk for adverse drug interactions, and a reassuring safety profile, emphasizing its suitability for oral administration. Crucially, molecular docking analyses revealed naringenin's capacity to engage multiple cancer-relevant targets with moderate to strong binding affinities, most notably CDK4, CDK6, Bcl-2, Bcl-xL, catalase, and NF-κB subunits. These results highlight its power to modulate crucial pathways in cell cycle control, apoptosis, oxidative stress regulation, and transcriptional signaling. The spectrum of intermolecular interactions, including hydrogen bonding, hydrophobic contacts, and aromatic stacking, suggests both stable and functionally significant ligand–protein complexes. Collectively, these findings position naringenin as a compelling natural lead for breast cancer drug development, capable of intervening in several hallmark oncogenic processes. While computational predictions provide strong mechanistic rationale and support for their pharmacological promise, future validation through molecular dynamics, in vitro bioassays, and translational studies remain essential. Naringenin thus stands out as an innovative candidate aligned with modern precision oncology efforts and the ongoing search for safe, effective, and multitarget anticancer therapies.

6. Disclosure Statements

6.1. Author Contribution

MV & SSJ: Writing – Original Draft Preparation; **KJ & SA:** Writing – Review and Editing; **CI, SI & SH:** Validation; **MR:** Conceptualization; Correction and Supervision. All the authors have read and approved the final manuscript.

6.2. Declaration of Generative AI

The authors declare that no generative AI tools were used in the drafting, writing, or editing of the manuscript. All scientific interpretations and conclusions are the author's own. AI-based tools were used only for language grammar refinement and formatting purposes, and the final content was verified and approved by the authors.

6.3. Ethics approval (for clinical/animal studies)

This study did not involve the participation of human subjects, the use of identifiable human data or tissue, or any experiments on live animals. Consequently, the requirement for ethical approval or informed consent did not apply.

6.4. Informed Consent Statement

Not applicable.

6.5. Data Availability Statement

The data that support the findings of this study are available from the corresponding author upon reasonable request.

6.6. Acknowledgment

We thank the Department of Science and Technology, Government of India, for providing support through the Fund for Improvement of S&T Infrastructure in Universities and Higher Educational Institutions (FIST) program (Grant No. SR/FIST/College-/2020/943).

6.7. Funding Statement

This research was funded by Department of Science and Technology (DST) Fund for Improvement of S&T Infrastructure in Universities and Higher Educational Institutions (FIST) program (Grant No. SR/FIST/College-2020/943).

6.8. Conflicts of Interest

The authors declare that they have no known financial, personal, academic, or other relationships that could inappropriately influence, or be perceived to influence, the work reported in this manuscript. All authors confirm that there are no competing interests to declare.

6.9. Corresponding Author Contact Information

The corresponding author **Dr. Manikkam Rajalakshmi** can be contacted via email rajalakshmi[at]hcctrichy.ac.in.

7. Reference

Ahmad, I., A. E. Kuznetsov, A. S. Pirzada, K. F. Alsharif, M. Daglia, and H. Khan. 2023. "Computational pharmacology and computational chemistry of 4-hydroxyisoleucine: Physicochemical, pharmacokinetic, and DFT-based approaches." *Front Chem* 11:1145974. doi: 10.3389/fchem.2023.1145974. PMID: 37123881.

Alamri, M. A., A. Altharawi, A. B. Alabbas, M. A. Alossaimi, and S. M. Alqahtani. 2020. "Structure-based virtual screening and molecular dynamics of phytochemicals derived from Saudi medicinal plants to identify potential COVID-19 therapeutics." *Arab J Chem* 13 (9):7224-7234. doi: 10.1016/j.arabjc.2020.08.004. PMID: 34909058.

Antypenko, L., K. Shabelnyk, O. Antypenko, M. Arisawa, O. Kamyshnyi, V. Oksenych, and S. Kovalenko. 2025. "In Silico Identification and Characterization of Spiro[1,2,4]triazolo[1,5-c]quinazolines as Diacylglycerol Kinase alpha Modulators." *Molecules* 30 (11). doi: 10.3390/molecules30112324. PMID: 40509212.

Anwar, S., J. Alanazi, N. Ahemad, S. Raza, T. A. Chohan, and H. Saleem. 2024. "Deciphering quinazoline derivatives' interactions with EGFR: a computational quest for advanced cancer therapy through 3D-QSAR, virtual screening, and MD simulations." *Front Pharmacol* 15:1399372. doi: 10.3389/fphar.2024.1399372. PMID: 39512829.

Brown, J. S., S. R. Amend, R. H. Austin, R. A. Gatenby, E. U. Hammarlund, and K. J. Pienta. 2023. "Updating the Definition of Cancer." *Mol Cancer Res* 21 (11):1142-1147. doi: 10.1158/1541-7786.MCR-23-0411. PMID: 37409952.

Carrington, E. M., Y. Zhan, J. L. Brady, J. G. Zhang, R. M. Sutherland, N. S. Anstee, R. L. Schenk, *et al.* 2017. "Anti-apoptotic proteins BCL-2, MCL-1 and A1 summate collectively to maintain survival of immune cell populations both in vitro and in vivo." *Cell Death Differ* 24 (5):878-888. doi: 10.1038/cdd.2017.30. PMID: 28362427.

Cord, D., M. C. Rimbu, and L. Popescu. 2025. "New prospects in oncotherapy: bioactive compounds from Taraxacum officinale." *Med Pharm Rep* 98 (3):290-299. doi: 10.15386/mpr-2875. PMID: 40786212.

Demian, M. D., V. I. Amasiorah, T. O. Johnson, and L. N. Ebenyi. 2024. "Phytochemical identification and in silico elucidation of interactions of bioactive compounds from Citrullus lanatus with androgen receptor towards prostate cancer treatment." *In Silico Pharmacol* 12 (1):27. doi: 10.1007/s40203-024-00193-5. PMID: 38596366.

Elsori, D., P. Pandey, S. Ramniwas, R. Kumar, S. Lakhanpal, S. O. Rab, S. Siddiqui, A. Singh, M. Saeed, and F. Khan. 2024. "Naringenin as potent anticancer phytocompound in breast carcinoma: from mechanistic approach to nanoformulations based therapeutics." *Front Pharmacol* 15:1406619. doi: 10.3389/fphar.2024.1406619. PMID: 38957397.

Gao, J., L. Yuan, H. Jiang, G. Li, Y. Zhang, R. Zhou, W. Xian, Y. Zou, Q. Du, and X. Zhou. 2024. "Naringenin modulates oxidative stress and lipid metabolism: Insights from network pharmacology, mendelian randomization, and molecular docking." *Front Pharmacol* 15:1448308. doi: 10.3389/fphar.2024.1448308. PMID: 39474612.

Ghayoor, A., and H. G. Kohan. 2024. "Revolutionizing pharmacokinetics: the dawn of AI-powered analysis." *J Pharm Pharm Sci* 27:12671. doi: 10.3389/jpps.2024.12671. PMID: 38433887.

Goodger, N. M., J. Gannon, T. Hunt, and P. R. Morgan. 1997. "Cell cycle regulatory proteins--an overview with relevance to oral cancer." *Oral Oncol* 33 (2):61-73. doi: 10.1016/s0964-1955(96)00071-1. PMID: 9231162.

Jain, A. N. 2009. "Effects of protein conformation in docking: improved pose prediction through protein pocket adaptation." *J Comput Aided Mol Des* 23 (6):355-374. doi: 10.1007/s10822-009-9266-3. PMID: 19340588.

Jiang, H., M. Zhang, X. Lin, X. Zheng, H. Qi, J. Chen, X. Zeng, W. Bai, and G. Xiao. 2023. "Biological Activities and Solubilization Methodologies of Naringin." *Foods* 12 (12). doi: 10.3390/foods12122327. PMID: 37372538.

Jung, W., S. Goo, T. Hwang, H. Lee, Y. K. Kim, J. W. Chae, H. Y. Yun, and S. Jung. 2024. "Absorption Distribution Metabolism Excretion and Toxicity Property Prediction Utilizing a Pre-Trained Natural Language Processing Model and Its Applications in Early-Stage Drug Development." *Pharmaceuticals (Basel)* 17 (3). doi: 10.3390/ph17030382. PMID: 38543168.

Karami, T. K., S. Hailu, S. Feng, R. Graham, and H. J. Gukasyan. 2022. "Eyes on Lipinski's Rule of Five: A New "Rule of Thumb" for Physicochemical Design Space of Ophthalmic Drugs." *J Ocul Pharmacol Ther* 38 (1):43-55. doi: 10.1089/jop.2021.0069. PMID: 34905402.

Kim, S., P. A. Thiessen, E. E. Bolton, J. Chen, G. Fu, A. Gindulyte, L. Han, *et al.* 2016. "PubChem Substance and Compound databases." *Nucleic Acids Res* 44 (D1):D1202-1213. doi: 10.1093/nar/gkv951. PMID: 26400175.

Kumar, M., M. Tomar, R. Amarowicz, V. Saurabh, M. S. Nair, C. Maheshwari, M. Sasi, *et al.* 2021. "Guava (*Psidium guajava* L.) Leaves: Nutritional Composition, Phytochemical Profile, and Health-Promoting Bioactivities." *Foods* 10 (4). doi: 10.3390/foods10040752. PMID: 33916183.

Li, X., Q. Jiang, and X. Yang. 2022. "Discovery of Inhibitors for Mycobacterium Tuberculosis Peptide Deformylase Based on Virtual Screening in Silico." *Mol Inform* 41 (3):e2100002. doi: 10.1002/minf.202100002. PMID: 34708566.

Lim, W., S. Park, F. W. Bazer, and G. Song. 2017. "Naringenin-Induced Apoptotic Cell Death in Prostate Cancer Cells Is Mediated via the PI3K/AKT and MAPK Signaling Pathways." *J Cell Biochem* 118 (5):1118-1131. doi: 10.1002/jcb.25729. PMID: 27606834.

Liou, G. Y., and P. Storz. 2010. "Reactive oxygen species in cancer." *Free Radic Res* 44 (5):479-496. doi: 10.3109/10715761003667554. PMID: 20370557.

Liu, T., L. Zhang, D. Joo, and S. C. Sun. 2017. "NF-kappaB signaling in inflammation." *Signal Transduct Target Ther* 2:17023-. doi: 10.1038/sigtrans.2017.23. PMID: 29158945.

Lok, B., D. Babu, Y. Tabana, S. S. Dahham, M. A. A. Adam, K. Barakat, and D. Sandai. 2023. "The Anticancer Potential of *Psidium guajava* (Guava) Extracts." *Life (Basel)* 13 (2). doi: 10.3390/life13020346. PMID: 36836712.

Lopez, G., I. Ezkurdia, and M. L. Tress. 2009. "Assessment of ligand binding residue predictions in CASP8." *Proteins* 77 Suppl 9 (Suppl 9):138-146. doi: 10.1002/prot.22557. PMID: 19714771.

Meng, X. Y., H. X. Zhang, M. Mezei, and M. Cui. 2011. "Molecular docking: a powerful approach for structure-based drug discovery." *Curr Comput Aided Drug Des* 7 (2):146-157. doi: 10.2174/157340911795677602. PMID: 21534921.

Moloney, J. N., and T. G. Cotter. 2018. "ROS signalling in the biology of cancer." *Semin Cell Dev Biol* 80:50-64. doi: 10.1016/j.semcdb.2017.05.023. PMID: 28587975.

Mukherjee, S., T. E. Balius, and R. C. Rizzo. 2010. "Docking validation resources: protein family and ligand flexibility experiments." *J Chem Inf Model* 50 (11):1986-2000. doi: 10.1021/ci1001982. PMID: 21033739.

Pellarin, I., A. Dall'Acqua, A. Favero, I. Segatto, V. Rossi, N. Crestan, J. Karimbayli, B. Belletti, and G. Baldassarre. 2025. "Cyclin-dependent protein kinases and cell cycle regulation in biology and disease." *Signal Transduct Target Ther* 10 (1):11. doi: 10.1038/s41392-024-02080-z. PMID: 39800748.

Pinzi, L., and G. Rastelli. 2019. "Molecular Docking: Shifting Paradigms in Drug Discovery." *Int J Mol Sci* 20 (18). doi: 10.3390/ijms20184331. PMID: 31487867.

Pires, D. E., T. L. Blundell, and D. B. Ascher. 2015. "pkCSM: Predicting Small-Molecule Pharmacokinetic and Toxicity Properties Using Graph-Based Signatures." *J Med Chem* 58 (9):4066-4072. doi: 10.1021/acs.jmedchem.5b00104. PMID: 25860834.

Ramirez, D., and J. Caballero. 2018. "Is It Reliable to Take the Molecular Docking Top Scoring Position as the Best Solution without Considering Available Structural Data?" *Molecules* 23 (5). doi: 10.3390/molecules23051038. PMID: 29710787.

Saleem, M., M. I. Qadir, N. Perveen, B. Ahmad, U. Saleem, T. Irshad, and B. Ahmad. 2013. "Inhibitors of apoptotic proteins: new targets for anticancer therapy." *Chem Biol Drug Des* 82 (3):243-251. doi: 10.1111/cbdd.12176. PMID: 23790005.

Salehi, B., P. V. T. Fokou, M. Sharifi-Rad, P. Zucca, R. Pezzani, N. Martins, and J. Sharifi-Rad. 2019. "The Therapeutic Potential of Naringenin: A Review of Clinical Trials." *Pharmaceuticals (Basel)* 12 (1). doi: 10.3390/ph12010011. PMID: 30634637.

Schirripa, A., V. Sexl, and K. Kollmann. 2022. "Cyclin-dependent kinase inhibitors in malignant hematopoiesis." *Front Oncol* 12:916682. doi: 10.3389/fonc.2022.916682. PMID: 36033505.

Venkataraman, M., G. C. Rao, J. K. Madavareddi, and S. R. Maddi. 2025. "Leveraging machine learning models in evaluating ADMET properties for drug discovery and development." *ADMET DMPK* 13 (3):2772. doi: 10.5599/admet.2772. PMID: 40585410.

Vinod, S. M., S. Murugan Sreedevi, A. Krishnan, K. Ravichandran, P. Karthikeyan, B. Kotteswaran, and K. Rajendran. 2023. "Complexity of the Role of Various Site-Specific and Selective Sudlow Binding Site Drugs in the Energetics and Stability of the Acridinedione Dye-Bovine Serum Albumin Complex: A Molecular Docking Approach." *ACS Omega* 8 (6):5634-5654. doi: 10.1021/acsomega.2c07111. PMID: 36816669.

Wong, F., A. Krishnan, E. J. Zheng, H. Stark, A. L. Manson, A. M. Earl, T. Jaakkola, and J. J. Collins. 2022. "Benchmarking AlphaFold-enabled molecular docking predictions for antibiotic discovery." *Mol Syst Biol* 18 (9):e11081. doi: 10.15252/msb.202211081. PMID: 36065847.

Xu, J., J. T. F. Wise, L. Wang, K. Schumann, Z. Zhang, and X. Shi. 2017. "Dual Roles of Oxidative Stress in Metal Carcinogenesis." *J Environ Pathol Toxicol Oncol* 36 (4):345-376. doi: 10.1615/JEnvironPatholToxicolOncol.2017025229. PMID: 29431065.

Yu, H., L. Lin, Z. Zhang, H. Zhang, and H. Hu. 2020. "Targeting NF-kappaB pathway for the therapy of diseases: mechanism and clinical study." *Signal Transduct Target Ther* 5 (1):209. doi: 10.1038/s41392-020-00312-6. PMID: 32958760.

Zafar, A., S. Khatoon, M. J. Khan, J. Abu, and A. Naeem. 2025. "Advancements and limitations in traditional anti-cancer therapies: a comprehensive review of surgery, chemotherapy, radiation therapy, and hormonal therapy." *Discov Oncol* 16 (1):607. doi: 10.1007/s12672-025-02198-8. PMID: 40272602.

How to Cite: Murugesan, V., Sathiya Jothi, S., Yasiha, K., Aishwariya, S., Ireen, C., Indu, S., Hinduja, S., & Rajalakshmi, M. (2025). Molecular docking analysis of Naringenin from the leaves of *Psidium guajava* as a promising agent for breast cancer therapy. Journal of Medico Informatics, 1(1), 35–43. Doi: http://doi.org/10.64659/jomi/210351